Silicon (2014) 6:117–121
DOI 10.1007/s12633-013-9176-9

ORIGINAL PAPER

Qualitative Evolution of Asymmetric Raman Line-Shape for NanoStructures

Rajesh Kumar · Gayatri Sahu · Shailendra K. Saxena · Hari M. Rai · Pankaj R. Sagdeo

Received: 25 September 2013 / Accepted: 17 December 2013 / Published online: 8 March 2014

Abstract A qualitative evolution of an asymmetric Raman line-shape function from a Lorentzian line-shape is discussed here for application in low dimensional semiconductors. The step-by-step evolution reported here is based on the phonon confinement model which is successfully used in literature to explain the asymmetric Raman line-shape from semiconductor nanostructures. Physical significance of different terms in the theoretical asymmetric Raman line-shape has been explained here. Better understanding of theoretical reasoning behind each term allows one to use the theoretical Raman line-shape without going into the details of theory from first principle. This will enable one to empirically derive a theoretical Raman line-shape function for any material if information about its phonon dispersion relation, size dependence, etc., is known.

Keywords Raman line-shape · Phonon scattering · Semiconductors · Nanostructures

Electronic supplementary material The online version of this article (doi:10.1007/s12633-013-9176-9) contains supplementary material, which is available to authorized users.

R. Kumar (✉) · G. Sahu · S. K. Saxena · H. M. Rai · P. R. Sagdeo
Discipline of Physics, School of Basic Sciences, Indian Institute of Technology Indore, Indore, Madhya Pradesh-452017, India
e-mail: rajeshkumar@iiti.ac.in

R. Kumar · P. R. Sagdeo
Disciplne of Surface Science and Engineering, Indian Institute of Technology Indore, Indore, Madhya Pradesh-452017, India

R. Kumar
Discipline of Bioscience and Bioengineering, Indian Institute of Technology Indore, Indore, Madhya Pradesh-452017, India

1 Introduction

Raman spectroscopy, since its discovery in 1928, is a technique which has been widely used to investigate the vibrational and electronic properties of materials [1, 2]. The crystalline, amorphous or nanocrystalline nature of any material can be ascertained by analysing its Raman scattering data. Raman spectroscopy provides a fast and convenient method to analyze the vibrational properties of crystalline and amorphous semiconductors [3–8].The physics behind Raman scattering in semiconductors or crystals is based on the inelastic interaction of incidence photons with lattice vibrations or phonons, that are sensitive to internal or external perturbations. In crystalline materials in the bulk form, the Raman scattering is limited to near zone centered phonons due to spectroscopic selection rules. But in the case of nanostructures, this selection rule gets relaxed and phonons other than the zone centered ones also contribute due to confinement of phonons in a crystallite of finite dimension [9–12]. This results in a change in the line-shape of the first order Raman spectrum which is typically Lorentzian for crystalline materials.

Line-shapes of Raman spectra from nano-structures are expected to be intermediate between those of the corresponding crystalline and amorphous materials. For example, a broad band around 470 cm^{-1} can be observed in the Raman spectra from amorphous Silicon (Si) [13] whereas at the other extreme of perfect crystalline Si, a sharp symmetric Lorentzian peak is observed at 521 cm^{-1} corresponding to the zone-centered phonon [14, 15]. In the case of Si nanostructures, there is a red-shift in Raman peak position and the line-shape also becomes broad and asymmetric compared to that of a bulk crystalline Si [11, 16–20]. The change in the Raman line-shape parameters (peak position, asymmetry and full width at half maxima or FWHM) is

useful in determining the size, shape and size distribution of nano-structures, since phonon softening and widening of Raman lines are related to the size of nanostructures. Attributing the observed asymmetric Raman line-shape from low dimensional material solely to quantum confinement may be misleading because the line-shape parameters are also dependent on temperature, stress, electron-phonon interaction, etc. A general concept to identify the confinement effect using Raman scattering must be understood. After this generalization, all the factors affecting the Raman line-shape can be taken care of by appropriately modeling the Raman line-shape equation for representation.

Asymmetric Raman line-shape from nanostructured semiconductors are often understood in the framework of the phonon confinement model (PCM) established by Richter et al. [21] and later modified by Campbell et al. [22]. This asymmetric Raman line-shape from nanostructures is mainly observed because the translational symmetry of the crystalline materials is broken at grain boundaries, which results in the appearance of specific surface and interface vibrational contributions [23]. This is more pronounced in reduced dimensional systems. These properties change the frequency of the phonons in the nanostructures, which is reflected in the Raman scattering. According to the PCM, intensity of the first-order Raman scattering can be written as Eq. 1

$$I_0(\omega) = \int_0^1 \frac{exp(-q^2L^2/4a^2)}{[\omega - \omega(q)]^2 + (\gamma/2)^2} d^n q, \quad (1)$$

where q is expressed in units of $2\pi/a$, a being the lattice constant, 0.543 nm. The parameter L stands for the average size of the nanocrystals. γ being the linewidth of the Si optical phonon in bulk c-Si (~ 4 cm^{-1}). 'n' shows the degree of confinement and may the take value of 2 or 3 for 2-dimensional or 3-dimensional confinement, respectively. Following Tubino et al. [24], the dispersion ω(q) of the optical phonon in a spherical Si nanocrystal can be taken as

$$\omega^2(q) = A + B\, cos\left(\frac{\pi q}{2}\right), \quad (2)$$

where $A = 1.714\times10^5$ cm^{-2} and $B = 1.000\times10^5$ cm^{-2}.

After close analyses of Eq. 1, one can say that it has evolved from a symmetric Lorentzian function with line-shape FWHM of 'γ'. However, Eq. 1 has been derived using quantum mechanical concepts, each term in Eq. 1 can be understood in terms of a concept without going into detailed mathematics. This will enable one to incorporate a particular perturbation by appropriately modifying Eq. 1 to get a Raman line-shape for the desired system. In the present study, we have discussed in depth, the evolution of an asymmetric Raman line-shape in nanomaterials starting from a symmetric Raman line-shape from its bulk counterpart. Understanding each term in the asymmetric Raman line-shape (due to phonon confinement effect) will enable the researchers to explore the possibility of the PCM beyond elemental semiconductor nanomaterials, like Si and Ge, and apply the same to other compound semiconductors like $GaAs$, TiO_2, etc. Although it is applicable to all the materials, in the present study we have done a detailed analysis of first-order Raman line-shape for Si nanostructures as an example.

2 Analysis and Discussion

As discussed earlier, the Raman line-shape is a manifestation of the Raman active phonon mode of a semiconductor obtained after scattering of light [23, 25]. It is an established fact that a Lorentzian Raman line-shape is observed from a bulk crystalline semiconductor, which is symmetric [23, 26, 27] in nature, whereas that from its nano counterpart is asymmetric [18–20, 28–31]. Figure 1a shows the longitudinal optic (LO) branch of phonon dispersion relation for Si. The discrete points in Fig. 1a shows the data reported in literature for the same [24, 32]. These data points can be represented theoretically as Eq. 2 [33–35].

Figure 1b shows a typical symmetric Raman line-shape from bulk Si represented by a Lorentzian line-shape and can be written as Eq. 3.

$$I_1(\omega) = \frac{1}{[\omega - \omega(0)]^2 + (\gamma/2)^2}, \quad (3)$$

where $\omega(0)$ is the zone center optical phonon frequency corresponding to q = 0 in Fig. 1a, and 'γ' is the FWHM of the Raman peak. For bulk Si, the values of $\omega(0) = 521$ cm^{-1} and $\gamma = 4$ cm^{-1}, are used to plot the Raman line-shape as shown in Fig. 1b. Since only phonons corresponding to q = 0 values participate in Raman scattering, a Lorentzian function with peak position at $\omega(0)$ is sufficient to represent the Raman line-shape from crystalline materials using Eq. 3.

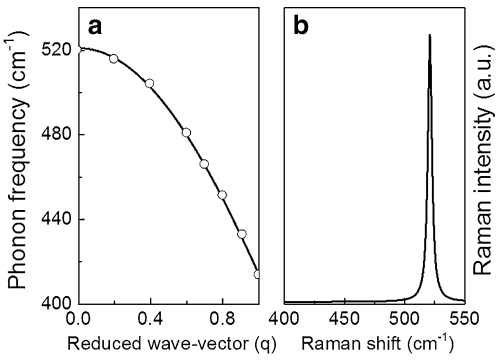

Fig. 1 **a** Longitudinal optic (LO) branch of phonon dispersion relation for silicon. The discrete points represent the experimental data reported by Tubino et al. [24]; **b** A typical Raman line-shape from bulk Si represented by Eq. 3

The Raman line-shape from nanostructured Si as given in Eq. 1 was derived by Richter et al. [21] and later modified by Campbell et al. [22]. All the terms in Eq. 1 represent a concept and is present with an underlying physics which will be discussed now. At nanoscale, phonons that participate in Raman scattering are confined within the boundary of the nanostructure. Due to the quantum confinement effect, breakdown of Raman selection rule takes place and phonons, away from the zone center ($q \neq 0$), also take part in the Raman scattering [21, 22] in addition to the zone centered ones. As a result, nonzero Raman intensities, $I_2(\omega)$, are also expected at lower frequencies (in wave-number units) away from $\omega(0)$. To represent this effect in a Raman line-shape function, Lorentzian line-shape corresponding to all frequencies (q = 0 to 1) on the phonon spectrum must be added together. After inclusion of this fact in Eq. 3, the Raman line-shape function can be written qualitatively as Eq. 4 as follows:

$$I_2(\omega) = \sum_q \frac{1}{[\omega - \omega(q)]^2 + (\gamma/2)^2}, \tag{4}$$

where summation over different values of q (varying from 0 to 1) represents the equal contributions from all the phonons. Since Eq. 4 involves a summation, variation in q (0 to 1) can be done in different steps. Raman line-shape in Eq. 4 is plotted in Fig. 2 for three different step sizes *viz*. 0.1, 0.05 and 0.02. It is important to mention here that the plots in Fig. 2 are not actual Raman line-shapes. Spikes in Fig. 2 correspond to the contribution in line-shape from individual phonon corresponding to a particular value of 'q' and are Lorentzian in nature with peak at a particular value of $\omega(q)$. For example, the peak marked with asterisk (*), centered at $\sim$ 414 cm^{-1}, represents the contribution of phonon represented by $q = 1$. For smaller step sizes, the line-shape is continuous instead of spiky as can be seen in Fig. 2c. The most important feature of the line-shape in Fig. 2c is its asymmetry as compared to the line-shape in Fig. 1b. A careful observation of the evolution from Fig. 2a–c reveals that an asymmetric line-shape arises if all phonons of a branch in phonon dispersion relation (Fig. 1a) take part in the Raman scattering with equal contributions. In addition to this it is also clear from Fig. 2 that spikes are prominent in the lower wavenumber region (400 − 475 cm^{-1}) as compared to the higher wavenumber region (475 − 521 cm^{-1}). This observation is directly related to the slope of the phonon dispersion relation in Fig. 1a. The phonon dispersion relation is almost flat near the zone center ($q = 0$), whereas it is monotonically decreasing near the zone edge ($q = 1$), making the dispersion relation nonlinear. Due to this nonlinearity, contributions from the phonons in the vicinity of the zone center add together to result in a higher intensity near 521 cm^{-1} (corresponding to $q = 0$ phonon frequency) forcing the line-shape function to become asymmetric. Line-shapes in Fig. 2 have been plotted by assuming that all the phonons from q = 0 to 1 contribute equally to the Raman intensity and the phonon wave-vector's values are discrete (as represented by steps in the value of q). The actual Raman line-shape from nanostructures can now be derived by taking into account the actual contribution from all the phonons and by taking continuous values of phonon wavevectors varying from zone-center to the zone-edge [22].

As discussed above, the actual asymmetric Raman line-shape (as observed from nanostructures) will be derived qualitatively here for the case of Si nanostructures. The contribution of the whole phonon spectrum in the Raman line-shape equation can be incorporated in Eq. 4 by integrating over the full dispersion relation rather than doing the sum-

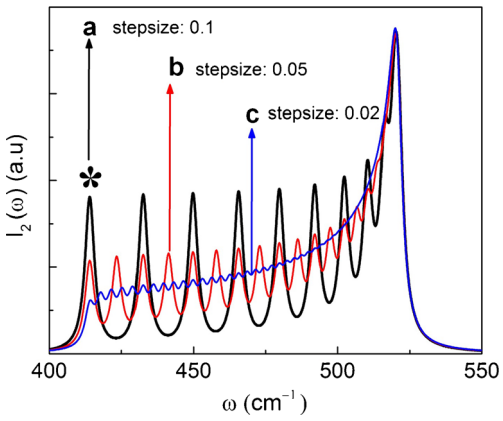

Fig. 2 Variation of Raman line-shape intensity as a function of wavenumbers plotted using Eq. 4. by considering contributions from optic phonons at different step sizes on the dispersion curve in Fig. 1a

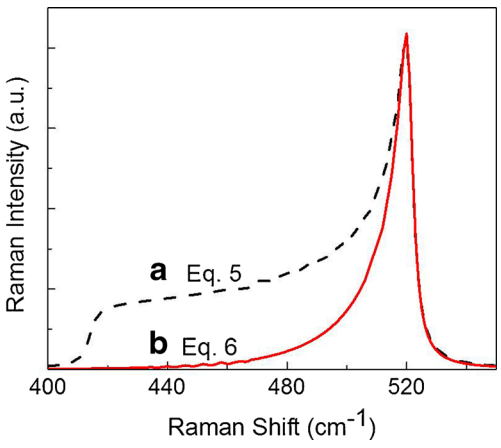

Fig. 3 Theoretical Raman line-shape function obtained by considering that all the phonons (from zone-center to zone-edge) take part in Raman scattering. Effect of size is not considered (**a**) whereas effect of size is considered (**b**)

mation as done in Eq. 3. As a result, the resultant line-shape equation can be written as Eq. 5 as follows.

$$I_3(\omega) = \int_0^1 \frac{1}{[\omega - \omega(q)]^2 + (\gamma/2)^2} dq \quad (5)$$

Equation 5 is plotted in Fig. 3a, where no spikes are seen in the asymmetric plot due to integration over all the possible values of q. Almost constant intensity in the $420 - 480$ cm^{-1} region is due to the hypothesis that all phonons contribute equally or have equal probability to participate in the Raman scattering. Since a nonzero Raman intensity away from $\omega(0)$ originates due to quantum confinement effect, the actual contribution of a phonon, in Raman scattering, depends on the extent of confinement inside a particular nanocrystal. This may be expressed quantitatively by introducing a weighting function [22] to take care of the actual contribution of a particular phonon. The nature of this weighting function depends on the dimensionality of confinement. For the simple case of spherical nanostructures, an exponential weighting function has been suggested by Campbell et al. [22] for all practical purposes. After introduction of the size dependence, the Raman line-shape is represented by Eq. 6 as follows:

$$I_4(\omega, L) = \int_0^1 \frac{exp(-q^2L^2/4a^2)}{[\omega - \omega(q)]^2 + (\gamma/2)^2} dq \quad (6)$$

where L is the size of the nanostructure and a is the lattice parameter of semiconductor crystal. Equation 6 is plotted by taking the value of $L = 2.5$ nm and $a = 0.543$ nm (lattice constant of Si) in Fig. 3b alongside Fig. 3a for comparison. By incorporating the size factor, the line-shape reflects the true asymmetric behavior as observed experimentally in the Raman spectra from nanostructures. Incorporation of the exponential term in Eq. 6 also takes care of the size dependence of the Raman line-shape, which is in consonance with the observed size dependent Raman scattering studies [11, 36–38]. Equation 6 can be understood as the basic Raman line-shape for nanostructured semiconductors in particular and nanostructured materials in general.

Modifications can be done in Eq. 6 to obtain various special Raman line-shapes reported to investigate the effects of stress, temperature, electron-phonon (Fano) effect, quantum confinement effect, etc. Details about these functions are available in the literature [33, 36, 39, 40], and is summarized in supplementary material also. Temperature dependence of phonon dispersion relation can directly be used in Eq. 6 if one wants to investigates the temperature dependent quantum confinement effects [41]. In addition, degree of confinement can also be considered by using the appropriate integral (surface or volume integral) and will result in Eq. 1 from where the discussion of this paper started. If, in a sample, all the nanostructures are not of the same dimension, a distribution function can successfully be introduced not only to take care of the distribution effect but also to know the exact size distribution available in the sample by theoretical fitting of the experimental data with the modified Raman line-shape.

3 Summary and Conclusions

An asymmetric Raman line-shape is observed from semiconductor nanostructures in contrast with a symmetric one from its bulk counterpart. This asymmetric line-shape is used to get information about the shape, size and distribution of nanostructures by theoretically fitting with a theoretical Raman line-shape function. An easy qualitative derivation of an asymmetric Raman line-shape from the symmetric Lorentzian function is suggested here. Different factors affecting the Raman line-shape have been incorporated mathematically in the Lorentzian line-shape function to obtain the asymmetric Raman line-shape for nanomaterials. Physical significance of different terms in the qualitatively derived asymmetric Raman line-shape have been explained for better consonance between theoretical Raman line-shape and experimental Raman scattering data. Better understanding of theoretical background makes the use of Raman line-shape function more versatile and can be used for other semiconductors and materials. If information about the phonon dispersion, size dependence, etc., is known, a Raman line-shape can be derived theoretically from the basic Lorentzian line-shape. Effects of other perturbations (like stress, temperature, etc.) can also be easily incorporated to get a new Raman line-shape.

Acknowledgments One of the authors (GS) would also like to acknowledge DST, Govt. of India, for the funding under DST Fast Track Scheme for Young Scientists, Project No. SR/FTP/PS-007/2012. Help from Mr. Ashish Kumar (IIT Indore) is also acknowledged.

References

1. Raman C (1928) A new radiation. Indian J Phys 02:387
2. Raman CV, Krishnan KS (1928) A new type of secondary radiation. Nature 121:501–502. doi:10.1038/121501c0
3. Barbagiovanni EG, Lockwood DJ, Simpson PJ, Goncharova LV (2012) Quantum confinement in Si and Ge nanostructures. J Appl Phys 111:034307. doi:10.1063/1.3680884
4. Ferrari AC, Robertson J (2000) Interpretation of Raman spectra of disordered and amorphous carbon. Phys Rev B 61:14095–14107. doi:10.1103/PhysRevB.61.14095
5. Ferrari AC, Robertson J (2001) Resonant Raman spectroscopy of disordered, amorphous, and diamondlike carbon. Phys Rev B 64:075414. doi:10.1103/PhysRevB.64.075414
6. Hultman L, Robertsson A, Hentzell HTG et al (1987) Crystallization of amorphous silicon during thinfilm gold reaction. J Appl Phys 62:3647–3655. doi:10.1063/1.339244

7. Vepek S, Iqbal Z, Sarott F-A (1982) A thermodynamic criterion of the crystalline-to-amorphous transition in silicon. Philos Mag Part B 45:137–145. doi:10.1080/13642818208246392
8. Shuker R, Gammon RW Raman-scattering selection-rule breaking and the density of states in amorphous materials. Phys Rev Lett 25:222. doi:10.1103/PhysRevLett.25.222
9. Sahu G, Joseph B, Lenka HP, Kuiri PK, Pradhan A, Mahapatra DP (2007) MeV Au irradiation induced nanoparticle formation and recrystallization in a low energy Au implanted Si layer. Nanotechnology 18:495702. doi:10.1088/0957-4484/18/49/495702
10. Sahu G, Mahapatra DP (2011) Raman scattering study of Si nanoclusters formed in Si through a double Au implantation. MRS Proceedings Spring Meeting 1354. doi:10.1557/opl.2011.1212
11. Sahu G, Kumar R, Mahapatra DP (2013) Raman Scattering and Backscattering Studies of Silicon Nanocrystals Formed Using Sequential Ion Implantation. Silicon 6:65. doi:10.1007/s12633-013-9157-z
12. Sahu G (2013) Raman scattering study on sequentially Au implanted sample. AIP Conf Proc 1536:293. doi:10.1063/1.4810216
13. Smith JE, Brodsky MH, Crowder BL et al (1971) Raman spectra of amorphous Si and related tetrahedrally bonded semiconductors. Phys Rev Lett 26:642–646. doi:10.1103/PhysRevLett.26.642
14. Temple PA, Hathaway CE (1973) Multiphonon Raman spectrum of silicon. Phys Rev B 7:3685–3697. doi:10.1103/PhysRevB.7.3685
15. Kumar R, Mavi HS, Shukla AK (2010) Spectroscopic investigation of quantum confinement effects in ion implanted silicon-on-sapphire films. Silicon 2:25–31. doi:10.1007/s12633-009-9033-z
16. Choi WK, Ng V, Ng SP et al (1999) Raman characterization of germanium nanocrystals in amorphous silicon oxide films synthesized by rapid thermal annealing. J Appl Phys 86:1398. doi:10.1063/1.370901
17. Serincan U, Kartopu G, Guennes A et al (2004) Characterization of Ge nanocrystals embedded in SiO2 by Raman spectroscopy. Semicond Sci Technol 19:247. doi:10.1088/0268-1242/19/2/021
18. Li B, Yu D, Zhang S-L (1999) Raman spectral study of silicon nanowires. Phys Rev B 59:1645–1648. doi:10.1103/PhysRevB.59.1645
19. Wang R, Zhou G, Liu Y et al (2000) Raman spectral study of silicon nanowires: high-order scattering and phonon confinement effects. Phys Rev B 61:16827–16832. doi:10.1103/PhysRevB.61.16827
20. Piscanec S, Cantoro M, Ferrari AC et al (2003) Raman spectroscopy of silicon nanowires. Phys Rev B 68:241312. doi:10.1103/PhysRevB.68.241312
21. Richter H, Wang ZP, Ley L (1981) The one phonon Raman spectrum in microcrystalline silicon. Solid State Commun 39:625–629. doi:10.1016/0038-1098(81)90337-9
22. Campbell IH, Fauchet PM (1986) The effects of microcrystal size and shape on the one phonon Raman spectra of crystalline semiconductors. Solid State Commun 58:739–741. doi:10.1016/0038-1098(86)90513-2
23. Gouadec G, Colomban P (2007) Raman spectroscopy of nanomaterials: how spectra relate to disorder, particle size and mechanical properties. Prog Cryst Growth Ch 53:1–56. doi:10.1016/j.pcrysgrow.2007.01.001
24. Tubino R, Piseri L, Zerbi G (1972) Lattice dynamics and spectroscopic properties by a valence force potential of diamond-like crystals: C, Si, Ge, and Sn. J Chem Phys 56:1022–1039. doi:10.1063/1.1677264
25. Bergman L, Nemanich RJ (1996) Raman spectroscopy for characterization of hard, wide-bandgap semiconductors: diamond, GaN, GaAlN, AlN, BN. Annu Rev Mater Sci 26:551–579. doi:10.1146/annurev.ms.26.080196.003003
26. Mavi HS, Islam SS, Kumar R, Shukla AK (2006) Spectroscopic investigation of porous GaAs prepared by laser-induced etching. J Non-Cryst Solids 352:2236–2242. doi:10.1016/j.jnoncrysol.2006.02.046
27. Mavi HS, Prusty S, Kumar M et al (2006) Formation of Si and Ge quantum structures by laser-induced etching. Phys Status Solidi A-Appl Mat 203:2444–2450. doi:10.1002/pssa.200521027
28. Pivac B, Furi K, Desnica D et al (1999) Raman line profile in polycrystalline silicon. J Appl Phys 86:4383. doi:10.1063/1.371374
29. Prusty S, Mavi HS, Shukla AK (2005) Optical nonlinearity in silicon nanoparticles: effect of size and probing intensity. Phys Rev B 71:113313. doi:10.1103/PhysRevB.71.113313
30. Konstantinovic MJ, Bersier S, Wang X et al (2002) Raman scattering in cluster-deposited nanogranular silicon films. Phys Rev B 66:161311. doi:10.1103/PhysRevB.66.161311
31. Piscanec S, Ferrari AC, Cantoro M et al (2003) Raman spectrum of silicon nanowires. Mater Sci Eng C 23:931–934. doi:10.1016/j.msec.2003.09.084
32. Brockhouse BN (1959) Lattice vibrations in silicon and germanium. Phys Rev Lett 2:256–258. doi:10.1103/PhysRevLett.2.256
33. Kumar R, Mavi HS, Shukla AK, Vankar VD (2007) Photoexcited Fano interaction in laser-etched silicon nanostructures. J Appl Phys 101:064315. doi:10.1063/1.2713367
34. Kumar R, Shukla AK (2009) Quantum interference in the Raman scattering from the silicon nanostructures. Phys Lett A 373:2882–2886. doi:10.1016/j.physleta.2009.06.005
35. Shukla AK, Kumar R, Kumar V (2010) Electronic Raman scattering in the laser-etched silicon nanostructures. J Appl Phys 107:014306. doi:10.1063/1.3271586
36. Kumar R, Shukla AK, Mavi HS, Vankar VD (2008) Size-dependent Fano interaction in the laser-etched silicon nanostructures. Nanoscale Res Lett 3:105–108. doi:10.1007/s11671-008-9120-x
37. Adu KW, Xiong Q, Gutierrez HR, Chen G, Eklund PC (2006) Raman scattering as a probe of phonon confinement and surface optical modes in semiconducting nanowires. Appl Phys. A 85:287–297. doi:10.1007/s00339-006-3716-8
38. Adu KW, Gutierrez HR, Kim UJ, Sumanasekera GU, Eklund PC (2005) Confined phonons in Si nanowires. Nanoletters 5:409–414. doi:10.1021/nl048625
39. Adu KW, Gutirrez HR, Kim UJ, Eklund PC (2006) Inhomogeneous laser heating and phonon confinement in silicon nanowires: a micro-Raman scattering study. Phys Rev B 73:155333. doi:10.1103/PhysRevB.73.155333
40. Gupta R, Xiong Q, Adu CK et al (2003) Laser-induced Fano resonance scattering in silicon nanowires. Nano Lett 3:627–631. doi:10.1021/nl0341133
41. Kumar R, Shukla AK (2008) Temperature dependent phonon confinement in silicon nanostructures. Phys Lett 373:133–135. doi:10.1016/j.physleta.2008.10.090